EMP Theoretical Notes

Note XVI
5 November 1965

The Compton Current

John S. Malik
Los Alamos Scientific Laboratory

Abstract

The present data relating to the Compton current produced by photons as a function of photon energy is estimated and presented in graphical form.

The Compton Current

An electron current results from collisions of gamma rays with air; this current is the major driving force of the emp. The dominant process in the energy range of interest is the Compton effect which is described by the Klein-Nishina relations; these are summarized in the appendix. Graphs of the Compton energy-angle relationships are presented by Nelms.[6] The differential cross-section per unit solid angle for scattering of the electron as a function of angle and gamma-energy are also presented in Fig. 1; the total and the absorption cross sections integrated over angle in Fig. 2; and the energy of the electron averaged over all angles in Fig. 3. These last two figures are from Nelms;[6] that report also contains Fig. 1 data in more detail.

The Compton electrons as produced move predominantly in the forward direction. As it traverses a material medium it dissipates its energy in a very large number of inelastic collisions, the net effect being a nearly continuous process. The theory for energy loss by inelastic encounters with electrons of the stopping material has been worked out by Bethe. For electrons of relatively low energy (less than the critical energy, 100 MeV for air) the energy loss is due to excitation and ionization of the bound electrons in the stopping material. The stopping power (dE/dx) is given by [3,8]

$$-\frac{dE}{dx} = \frac{2\pi\, r_e^2\, mc^2\, NZ}{\beta^2} \left\{ \log\left[\frac{\tau(\tau+2)}{2\,(I/mc^2)^2}\right] + 1 - \beta^2 + \left[\tau^2/8 - (2\tau+1)\ \log 2\right] / (\tau+1)^2 \right\} \quad \text{MeV/cm}$$

where

mc^2 = rest energy = 0.511 MeV

τ = kinetic energy of electron in units of mc^2

NZ = number of electrons / cm^3

$r_e^2 = (e^2/mc^2)^2$

I = excitation energy ($\sim$ 87 ev for air)

An extensive set of calculations applying this theory to several materials has been prepared by Nelms,[7] and by Berger and Seltzer.[11] These works tabulate the stopping power (-dE/dx) and the reciprocal stopping power (RSP) (or continuous-slowing-approximation [csda]) range,

$$R_{RSP} = \int_0^T \left(- \frac{dE}{dx} \right)^{-1} dE$$

for many materials; the data for aluminum and for air are shown in Figs. 4,5. This range, while a definite quantity, is not physically realizable mainly because of elastic collisions of the electron with the atom in which the electron is merely deflected without loss of energy. The theory of multiple scattering is discussed by Bethe, Ashkin.(2) The work of Williams(9) quoted in(2) shows the mean square angle of scattering involves the logarithm of $Z^{4/3}/A$ and hence is rather insensitive to the material. With this observation, scattering results for aluminum might be expected to be applicable to air. Experimental data for the "practical" range of electrons in aluminum are summarized by Katz, Penfold(12), quoted in the American Institute of Physics Handbook, and shown in Fig. 1. This range is about 0.80 of the csda range calculated by Nelms(7) or Berger.(11) The calculated csda range in air is about 0.90 that for aluminum.

Intensity versus range data for aluminum measured by Marshall and Ward,(10) and quoted by Bethe and Ashkin and by Birkhoff(3) show the range at half intensity to be about 0.66 the extrapolated range. (The half intensity point is the value given by multiple scattering theory to derive the average range.) The average value based upon total area is about 0.68 of the extrapolated value. Longmire used the value 2/3 in his Lecture notes on emp; AFWL used the value 0.63. The value to be adopted for this work is 2/3.

To provide further information upon the value to use for average range, Martin Walt of Lockheed performed a diffusion calculation of electrons produced by 2 MeV gamma rays incident upon a slab of air. The calculation assumes that the electrons interact with air through shielded Coulomb collisions with the energy loss-rate given by the Bethe dE/dx relation. The numerical solution involves starting at the highest energy, using implicit finite difference methods to sweep through the spatial and angular mesh in the direction of current flow, eventually returning to the outer boundary. The integration scheme is similar to the S_n method of Carlson. The numerical integration scheme requires that the energy distribution be peaked in the forward direction and hence it was not possible in these calculations to use the proper angle-energy relationships appropriate to Compton scattering. Two calculations were made: one calculation used the proper angle dependence but with all electrons having a value near 1.76 MeV which is the maximum possible (the average is about 1 MeV); this gave plausible intensity distance and energy dependence with an average range of 0.55 gm/cm^2. The second calculation used the proper energy distribution but with all electrons directed forward; this yielded an average range of 0.36 gm/cm^2. Both are high as expected considering the starting assumptions. They lend credence however to the use of the Marshall, Ward data for the multiple scattering correction.

To derive a relationship for the average range of the Compton resulting from gamma ray interaction with air, the same procedure used by Longmire was followed. The range data from Fig. 5 was fit by the relation:

$$R_{csda} = \frac{.61E^2}{E + .26} \quad gm/cm^2$$

with E in MeV. To arrive at the average forward range for the electron it is multiplied by cos ϕ to get the forward component, by 0.8 to get the practical range, and by 2/3 for the average range. This is then averaged over all possible angles for Compton scattering to arrive at the mean forward range:

$$R_{MF} = \frac{.533 \int \frac{d\sigma}{d\Omega} R_{csda} \cos\phi \, d\Omega}{\int \frac{d\sigma}{d\Omega} \, d\Omega}$$

The result is shown in Fig. 6. Also shown in Fig. 6 is the ratio of this range to the gamma mean free path for production of Compton electron and also the quantity

$$\frac{R_{MF} \lambda_a}{E_\gamma \lambda_t} \quad gm/cm^2 \ MeV$$

which is the gamma energy dependent part of the saturation electric field relation. It may be seen that while the ratio R_{MF}/λ_t is not constant, the second relationship is sensibly constant over the energy range of interest.

The nearly empirical determination of the Compton electron range indicates a need for further work in this area, both theoretical and experimental. The multiple scattering corrections for both practical and average ranges are based primarily on data which may not be as directly applicable to a spectrum of electron energies as is implied here and a more complete calculation would be worth while. There exist no good experimental data on electron ranges nor of Compton electron ranges in air; electron range data for aluminum do exist but the corresponding data for Compton electron ranges are questionable. The errors in the ranges predicted here are probably not large but the prediction is not satisfying.

References:

1. W. Heitler, Quantum Theory of Radiation, Oxford Press, London, 1954.
2. H. A. Bethe, J. Ashkin, in Experimental Nuclear Physics edited by E. Segrè, Vol I, pt II-2, John Wiley & Sons, New York, 1953.
3. R. D. Birkhoff, Handbuch der Physik, Band XXXIV, pp. 54-138, Springer-Verlag, Berlin, 1958.
4. C. M. Davisson, R. D. Evans, Gamma Ray Absorption Coefficients, Revs. Mod. Phys., 24, 79 (1952).
5. R. D. Evans, Compton Effect, Handbuch der Physik, Band XXXIV, p. 218-298, Springer-Verlag, Berlin, 1958.
6. A. T. Nelms, Graphs of the Compton Energy-Angle Relationship and the Klein-Nishina Formula from 10 KeV to 500 MeV, NBS Circular 542, U.S. Government Printing Office, 1953.
7. A. T. Nelms, Energy Loss and Range of Electrons and Positrons, NBS Circular 577 (1956) and Supplement to NBS Circular 577 (1958), U. S. Government Printing Office.
8. R. Rohrlich, B. C. Carlson, Positron-Electron Differences in Energy Loss and Multiple Scattering, Phys. Rev., 93, 38 (1954).
9. E. J. Williams, Concerning the Scattering of Fast Electrons and of Cosmic-Ray Particles, Proc. Roy. Soc. (London) A169, 531 (1939).
10. J. S. Marshall, A. G. Ward, Absorption Curves and Ranges for Homogeneous β-rays. Can. J. Res. A15, 39 (1937).
11. M. J. Berger, S. M. Seltzer, Tables of Energy Losses and Ranges of Electrons Positrons, NASA SP-3012, NASA Washington D. C., 1964. Part of NAS-NRC Publication 1133, to be published.
12. L. Katz, A. S. Penfold, Revs. Mod. Phys. 24, 28 (1952).

APPENDIX:

Compton effect relationships:

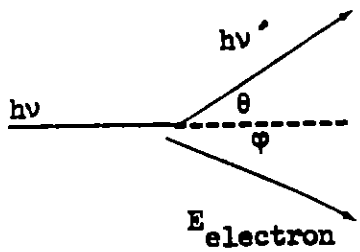

$$\alpha = \frac{h\nu}{m_o c^2}$$

$$\alpha' = \frac{h\nu'}{m_o c^2}$$

$$\alpha' = \frac{\alpha}{1 + \alpha\,(1 - \cos\theta)}$$

$$E_{electron} = m_o c^2 \left(\frac{2\alpha^2}{1 + 2\alpha + (1+\alpha)^2\ \tan^2\varphi} \right) = m_o c^2\ \frac{\alpha^2\ (1 - \cos\theta)}{1 + \alpha\ (1 - \cos\theta)}$$

$$\cos\theta = 1 - \frac{2}{(1+\alpha)^2 \tan^2\varphi + 1}$$

$$\tan\varphi = \frac{\sin\theta}{(1+\alpha)\ (1 - \cos\theta)} = \frac{1}{(1+\alpha)}\ \text{ctn}\ \frac{\theta}{2}$$

Cross section for the number of photons scattered per electron per unit solid angle in direction θ :

$$\frac{d_e\sigma(\theta)}{d\Omega} = \frac{r_o^2}{2} \left\{ \frac{1}{[\ 1 + \alpha\ (1 - \cos\theta)\ ]^2} \left[1 + \cos^2\theta + \frac{\alpha^2\ (1 - \cos\theta)^2}{1 + \alpha\ (1 - \cos\theta)} \right] \right\}$$

Cross section for the number of electrons scattered per electron per unit solid angle in direction φ :

$$\frac{d_e\sigma(\varphi)}{d\Omega_\varphi} = \frac{d_e\sigma(\theta)}{d\Omega_\theta} \cdot \frac{d\Omega_\theta}{d\Omega_\varphi}$$

$$\frac{d\Omega_\theta}{d\Omega_\varphi} = \frac{-\,4\ (1+\alpha)^2\ \cos\varphi}{[\ (1+\alpha)^2 - \alpha(\alpha+2)\ \cos^2\varphi]^2} = \frac{-\,4\ (1+\alpha)^2\ \cos\varphi}{[\ 1 + \alpha\ (\alpha+2)\ \ \sin^2\varphi]^2}$$

$$r_o = \frac{e^2}{m_o c^2} = 2.8182.10^{-13}\ \text{cm}$$

$$4r_o^2 = 0.3177\ \text{b}$$

$$\frac{d_e\sigma(\varphi)}{d\Omega_\varphi} = r_e^2 \left\{ \frac{4\,(1+\alpha)^2 \cos\varphi}{\left[1+\alpha\,(\alpha+2)\sin^2\varphi\right]\left[1+2\alpha+\alpha^2\sin^2\varphi\right]^2} \left[\frac{\cos^4\varphi+(\alpha+1)^4\sin^4\varphi}{1+\alpha\,(\alpha+2)\sin^2\varphi}+\frac{2\,\alpha^2\cos^4\varphi}{1+2\alpha+\alpha^2\sin^2\varphi}\right]\right\}$$

or

$$r_e^2 \left\{ \frac{4\,(1+\alpha)^2 \cos\varphi}{\left[1+(\alpha+1)^2\tan^2\varphi\right]\left[1+2\alpha+(\alpha+1)^2\tan^2\varphi\right]^2} \left[\frac{1+(\alpha+1)^4\tan^4\varphi}{1+(\alpha+1)^2\tan^2\varphi}+\frac{2\,\alpha^2}{1+2\alpha+(\alpha+1)^2\tan^2\varphi}\right]\right\}$$

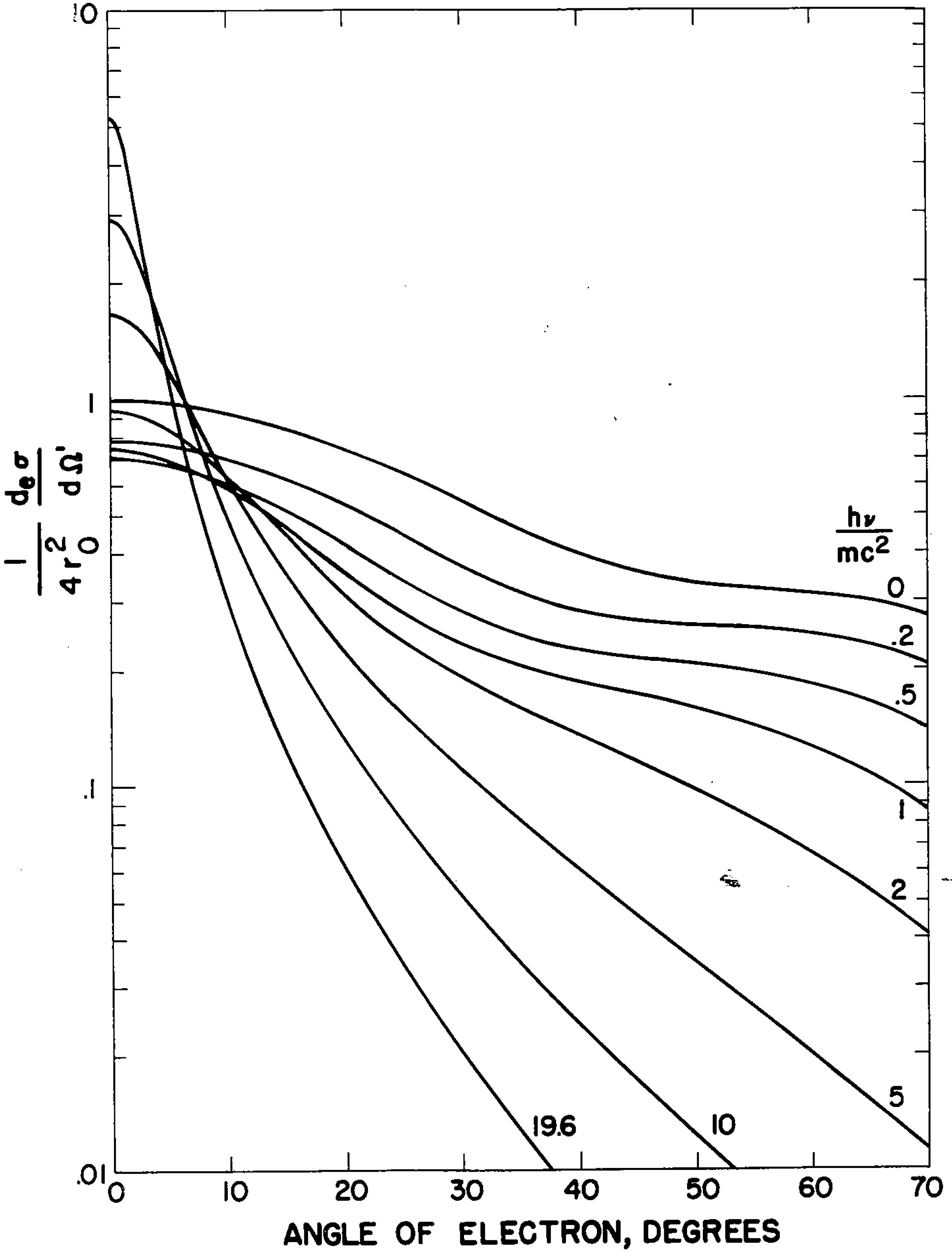
10
1
.1
.01
$\frac{1}{4r_0^2}\frac{d_e\sigma}{d\Omega'}$
$\frac{h\nu}{mc^2}$
0
.2
.5
1
2
5
10
19.6
0
10
20
30
40
50
60
70
ANGLE OF ELECTRON, DEGREES
FIG. 1

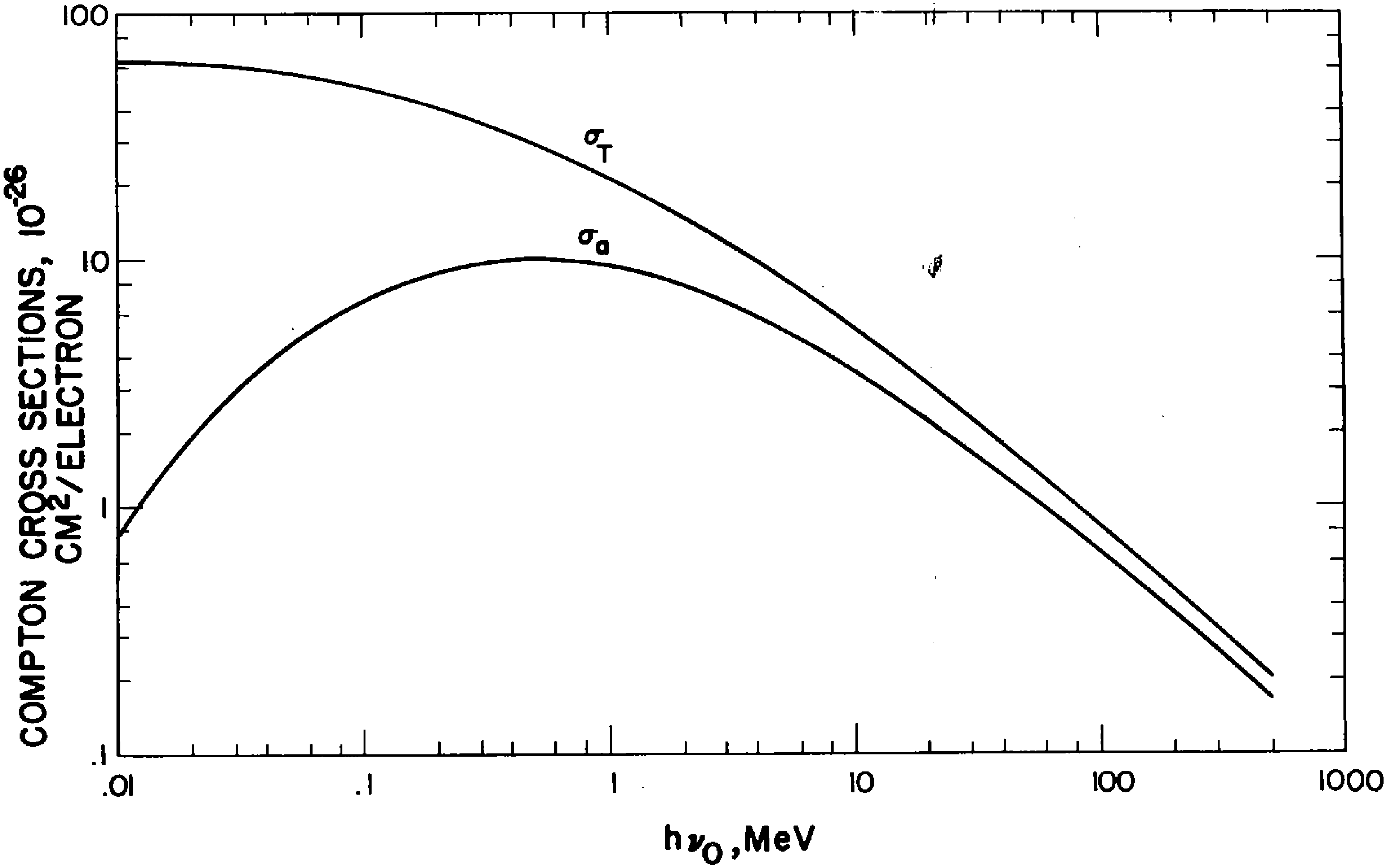

COMPTON CROSS SECTIONS, 10^{-26} CM^2/ELECTRON
100
10
1
.1
σ_T
σ_a
.01
.1
1
10
100
1000
$h\nu_0$, MeV

FIG. 2

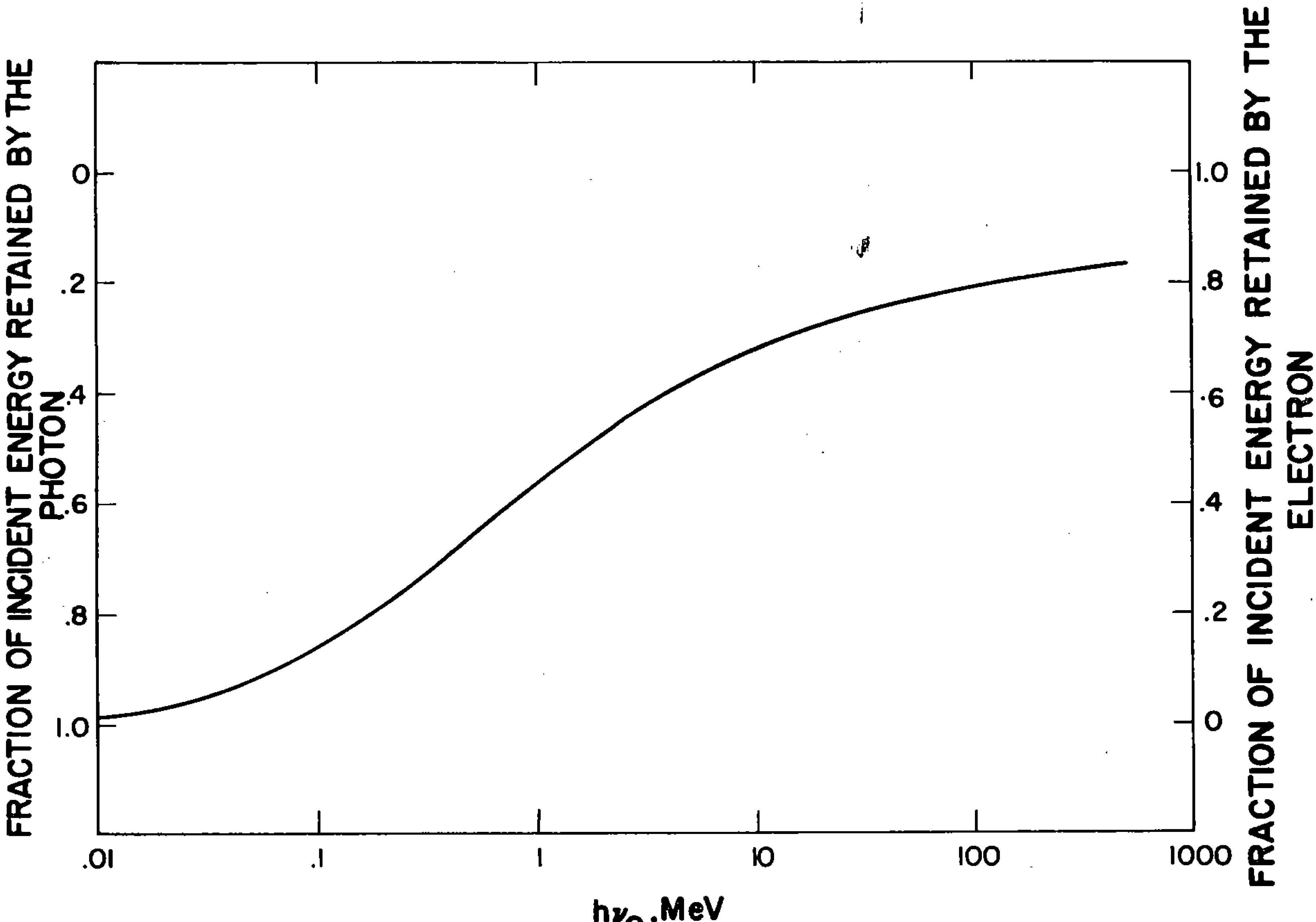

FRACTION OF INCIDENT ENERGY RETAINED BY THE PHOTON
0
.2
.4
.6
.8
1.0
FRACTION OF INCIDENT ENERGY RETAINED BY THE ELECTRON
1.0
.8
.6
.4
.2
0
.01
.1
1
10
100
1000
hν0, MeV

FIG. 3

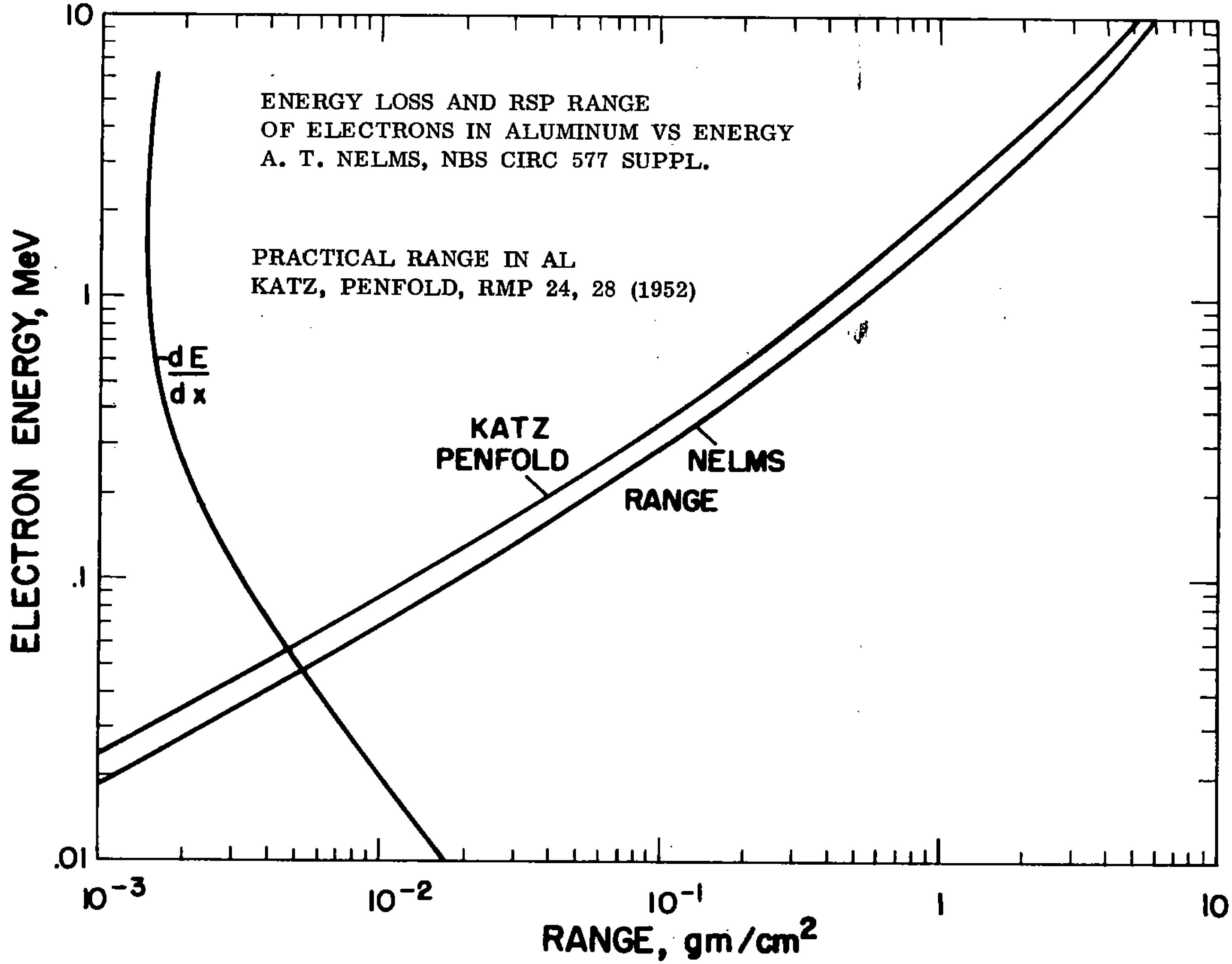

ENERGY LOSS AND RSP RANGE
OF ELECTRONS IN ALUMINUM VS ENERGY
A. T. NELMS, NBS CIRC 577 SUPPL.
PRACTICAL RANGE IN AL
KATZ, PENFOLD, RMP 24, 28 (1952)
-dE/dx
KATZ
PENFOLD
NELMS
RANGE
ELECTRON ENERGY, MeV
10
1
.1
.01
10^-3
10^-2
10^-1
1
10
RANGE, gm/cm2

FIG. 4

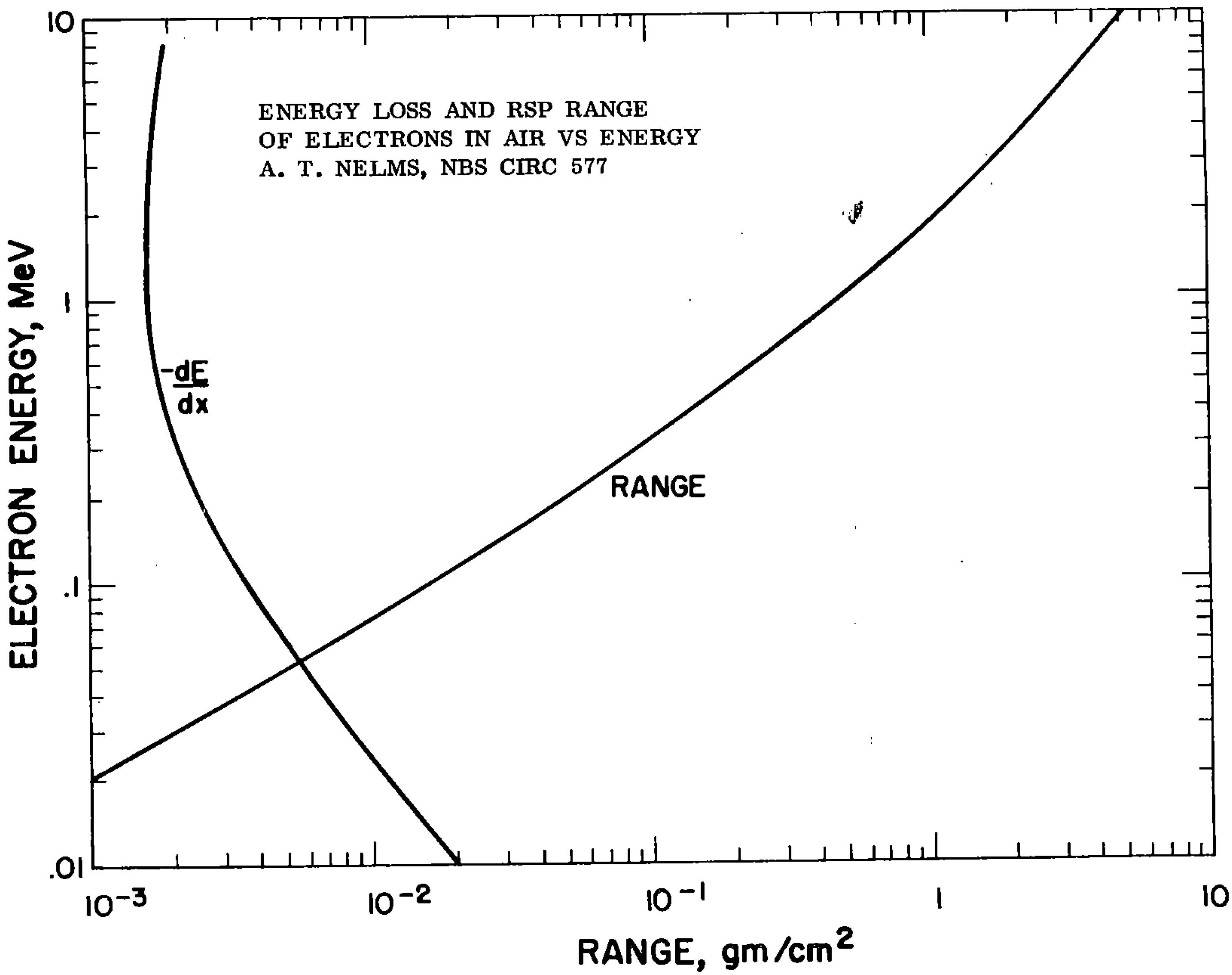
ENERGY LOSS AND RSP RANGE
OF ELECTRONS IN AIR VS ENERGY
A. T. NELMS, NBS CIRC 577
-dE/dx
RANGE
10
1
.1
.01
ELECTRON ENERGY, MeV
10^-3
10^-2
10^-1
1
10
RANGE, gm/cm^2

FIG. 5

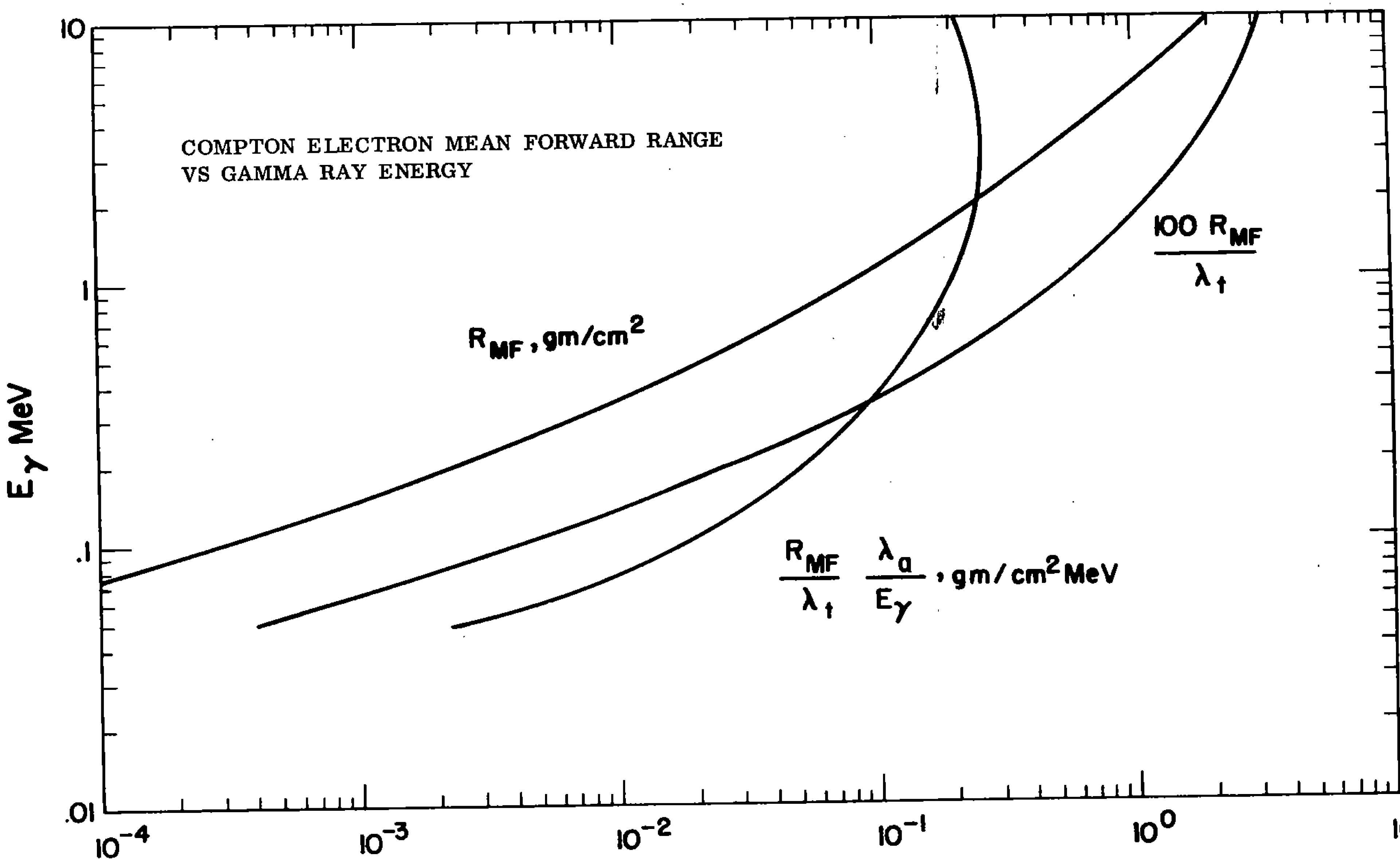

COMPTON ELECTRON MEAN FORWARD RANGE
VS GAMMA RAY ENERGY
E_γ MeV
10
1
.1
.01
R_{MF}, gm/cm²
$\frac{100\ R_{MF}}{\lambda_t}$
$\frac{R_{MF}}{\lambda_t}\ \frac{\lambda_a}{E_\gamma}$, gm/cm² MeV
10^{-4}
10^{-3}
10^{-2}
10^{-1}
10^{0}
10^{1}

FIG. 6